Progressive Evolution and a Measure for its Noise-dependent Complexity

Siegfried Fussy, Gerhard Grössing, and Herbert Schwabl

Austrian Institute for Nonlinear Studies,
Parkgasse 9, A-1030 Vienna, Austria
email: ains@teleweb.at, siegfried.fussy@eudoramail.com
http://web.telekabel.at/ains/, fax: +43 1 7150177

Abstract

A recently introduced model of macroevoluton is studied on two different levels of systems analysis. Firstly, the systems dynamics and properties, above all the growth of complexity of the evolutionary units during the long-term evolution, are discussed, and, secondly, the complexity of the model itself, i.e. the richness of its various features, is studied with regard to a control parameter representing a background noise within the systems dynamics. The same is done with a randomized version of the model.

The model is based on a normalized one-dimensional coupled map lattice with locally interacting sites representing different species. The evolution of the sites' values representing the fitness of the species is governed by a usual diffusion rule and an additional memory- or random-based feedback loop. The introduction of a realistic background noise limiting the range of the feedback operation yields a pattern signature in fitness space with a distribution of temporal boost/mutation distances similar to a punctuated equilibrium behavior. Furthermore, the behavior of the mean lifetimes of "high" fitness values is correlated with the resolution-like parameter ε via a power law, a phenomenon called "fractal evolution". Based on simple functional properties of the power law, an additional feedback loop is introduced to use the intrinsic fluctuations of the whole fitness landscape as a driving force to change adaptively the systems resolution. On long-term scales, the dynamical system properties exhibit a clear tendency towards progressive evolution potentials for each species.

For both model versions, the memory-based and the random-based one, we achieve some basic mechanisms of evolutionary dynamics like coevolution, punctuated equilibrium with regard to internal or external changes during evolution, coordinated stasis for groups of species, and self-organized growth of complexity for all evolutionary units of the array leading to a kind of "Red-Queen-effect" Additionally, for the memory based model a parameter was found indicating a limited range of noise allowing for the most complex behavior of the model, whereas the entropy of the system provides only a monotonous measure with respect to the varying noise level.

Keywords: macroevolution, punctuated equilibrium, complexity, fractal evolution, background noise

1. Introduction

There exists a long and ongoing discussion among the evolution theorists whether or not biological evolution can be characterized by an increase of complexity of some evolutionary units. This scenario, also called "progressive evolution" (Gordon, 1998) is accompanied by an "arrow of time" characterizing an irreversible growth of complex biological features like ,e.g., the evolution from monocellular organisms to multicellular ones, the development of a nerve system and the building of social structures with division of labor. Besides the fundamental problem of agreeing upon a commonly accepted definition of "biological complexity" (Smith and Szathmáry,

1997), both of the extreme positions, i.e., a quasi teleological one with a necessary evolutionary trend towards humans as most complex "output" of evolution on one hand, and a complete absence of any trend within evolution on the other, seem to be hard to maintain.

Within a more differentiated scenario it has been argued (Gould, 1996) that the appearance of the "common sense" complex features mentioned above were not based on a general progressive trend but on chance, just as a consequence of increasing variance. Since a wall of "minimal complexity" of living entities (represented by bacteria) prevents the expansion to still less complex species, the trendless random process necessarily spreads to higher complexity thereby pretending progressive trend.

We think that a probable absence of a general evolutionary trend towards increasing complexity is no necessary contradiction to the concept of progressive evolution. Even if the overwhelming majority of organisms remained on a level once achieved just appropriate to survive even for billions of years, some ratchet-like self-organized mechanisms could account for the further evolution of a probably small number of species within the phylogenetic tree. Concerning microevolution, i.e. evolution at the microscopic biological level, a lot of mechanisms for self-organized processes leading to complex structures and organisations have been developed and analyzed (e.g., Kauffmann, 1993; Schuster, 1994; Gordon, 1998).

On the "macroscopic" level of macroevolution some of its qualitative features like punctuated equilibrium have been successfully simulated by Bak and Sneppen (1993) in a toy model on a one-dimensional lattice of sites, with each site representing a species, thereby drawing on earlier work on self-organized criticality (SOC) (Bak *et al*., 1987, 1988). However, as their model allows to add together only accumulated mutations at single sites, i.e., without differentiating between progress and regression in fitness over time, the accumulated activity pattern is also time-invariant. Despite of further improvements (Vandewalle and Ausloos, 1995; Solé and Manrubia, 1996) one important question is hardly touched upon by these models, namely how evolution produces entities of increased complexity. For, the SOC state seems to represent always a "quasi - steady state", i.e., the only trend within the evolution process is to self-organize into the same critical steady state having, as a consequence, the same appearance because of the models' inherent time symmetry (at least at large time scales).

The following model of macroevolution tries to integrate some basic features of evolutionary dynamics like coevolution, punctuated equilibrium with regard to internal or external changes (mutations, catastrophes) during evolution, coordinated stasis for groups of species, and a basic, time symmetry breaking mechanism allowing for self-organized growth of complexity for the evolutionary units taken into consideration.

2. Fractal and Progressive Evolution

In this section a simplified version of a recently introduced model of macroevolution (Fussy *et al*., 1997), i.e. evolution on the population/species level, and a randomized analogon, are presented and analyzed.

Said units are described by a one-dimensional array of cells with fitness values $0 \le \rho_0(t,j) \le 1$ and with $j = 1,...,N$ representing the number of species on a coupled map lattice (CML). Their (co-) evolution in time is constrained to nearest neighbor interaction of the form

$$\rho_0(t,j) = \frac{1}{N_0(t)}\left\{\rho_0(t-1,j) + \delta\left[\rho_0(t-1,j-1) + \rho_0(t-1,j+1)\right]\right\}$$

$$j = 1,...,N, \qquad \rho_0, \delta \in \Re$$

(1)

with δ as coupling constant quantifying the nearest neighbor interaction and N_0 as normalization factor yielding

$$\sum_{j=1}^{N} \rho_0(t,j) = 1 \quad \text{for all } t.$$

(2)

To take into account the ever existing background noise coming from internal and/or external fluctuations, a system's internal precision limit ξ_{max} is introduced, which is chosen for the time being as $\xi_{max} = 10^{-6}$. In effect, each site $\rho_0(t,j) \le \xi_{max}$ is replaced by a white noise term, generated by $\xi_{max} \cdot RAN$. The random number RAN is uniformly distributed on the interval [0, 1]. In Section 3, ξ_{max} is used as control parameter and varied within a range of almost 40 orders of magnitude to analyze the correspondingly changing properties of the systems dynamics.

In this way, $\rho_0(t)$ assumes values between zero and one representing the individual species' fitness at time step *t* relative to the others in such a manner that the total fitness for the whole array is given by a constant which, without loss of generality, is defined to be equal to unity. Contrary to the method of eliminating the least fit species as in Bak and Sneppen (1993) we concentrate on the generation of high fitness values and their further evolution.

2.1 Memory-Based Evolution

In a next step, a temporal feedback loop is introduced in the first version of our model representing a certain periodicity of constraining conditions for the whole evolutionary landscape. For a detailed discussion about motivation and interpretation, we refer to Fussy *et al.* (1997) and to Robertson and Grant (1996).

To implement said temporal feedback operation in our model of Eq. (3), we install an enhancement (of strength A_{amp}) of each site $\rho(t,j) > \xi_{max}$ fulfilling an ε-condition

$$\rho(t,j) = \frac{1}{N(t)} \left(\left[A_{amp} - \rho_{0,\xi}(t,j) \right] \cdot \theta_\varepsilon \cdot \theta_{mem} \cdot \theta_\xi + \rho_{0,\xi}(t,j) \right)$$

with

$$\rho_{0,\xi}(t,j) = \left[\rho_0(t,j) - \xi \right] \cdot \theta_\xi + \xi, \; \rho_0(t,j) \text{ defined in Eq. (1)},$$

$$\xi = \xi_{max} \cdot RAN, \; RAN \in [0,1], \; \theta_\xi = \Theta \left(\rho_0(t,j) - \xi_{max} \right),$$

$$\theta_\varepsilon = \Theta \left(\varepsilon - \left| \frac{\rho_{0,\xi}(t,j)}{\rho(t - t_{mem}, j)} - 1 \right| \right), \; 0 \le \varepsilon \le 1 \, (= 100\%), \; \theta_{mem} = \Theta \left(t - t_{mem} \right),$$

$$\text{and } \Theta(x) = \begin{cases} 1: & x > 0 \\ 0: & x \le 0. \end{cases}$$

(3)

As usual, we impose periodic boundary conditions. Also, we introduce a time span t_{mem} during which the system's memory is effective.

In other words, the enhancement for any site $\rho_{0,\xi}(t,j) > \xi_{max}$ takes place if $t > t_{mem}$ (i.e., the time span during which a system's memory is effective) and if the condition $\rho(t - t_{mem}, j) \cdot (1 - \varepsilon) < \rho_{0,\xi}(t,j) < \rho(t - t_{mem}, j) \cdot (1 + \varepsilon)$ is fulfilled. Note that this kind of feedback operation simulates a selection process enhancing the values and, consequently, the further evolutions of those sites which are comparable in fitness with their corresponding values in the past since they fulfill the ε-condition.

The whole normalized system is constrained to the range $0 \le \rho(t,j) \le 1$. Values of $\rho(t,j) \le \xi_{max}$ are, just for simplicity, replaced by white noise terms, i.e., in that case, whatever kind of noise that exists in our system exceeds a signal generated by the system's rules. The domain of "high" fitness is described by the threshold value $L \gg \xi_{max}$. Although the actual choice of L seems to be somewhat arbitrary, it turns out in the following that the relevant system properties are not concerned by this choice.

Summarizing all the parameter values used in the following analysis, we use for our "default model"

Number of sites (dimension) $N = 120$

Inintial values (before normalization) $\rho(0,40) = 0.1, \rho(0,60) = 0.9, \rho(0,100) = 0.3$

Mixing parameter (coupling constant) $\delta = 0.03$

Boost value (enhancement) $A_{amp} = 100$ (4)

Size of memory $t_{mem} = 300$

Threshold value for high fitness domains $L = 10^{-2}$

Maximal background noise $\xi_{max} = 10^{-6}$.

All relevant system properties like punctuated equilibrium or fractal evolution remain stable under variation of the parameters listed above (cf. Fussy *et al.,* 1997) except for variation of the noise threshold ξ_{max} which is discussed in Section 3.
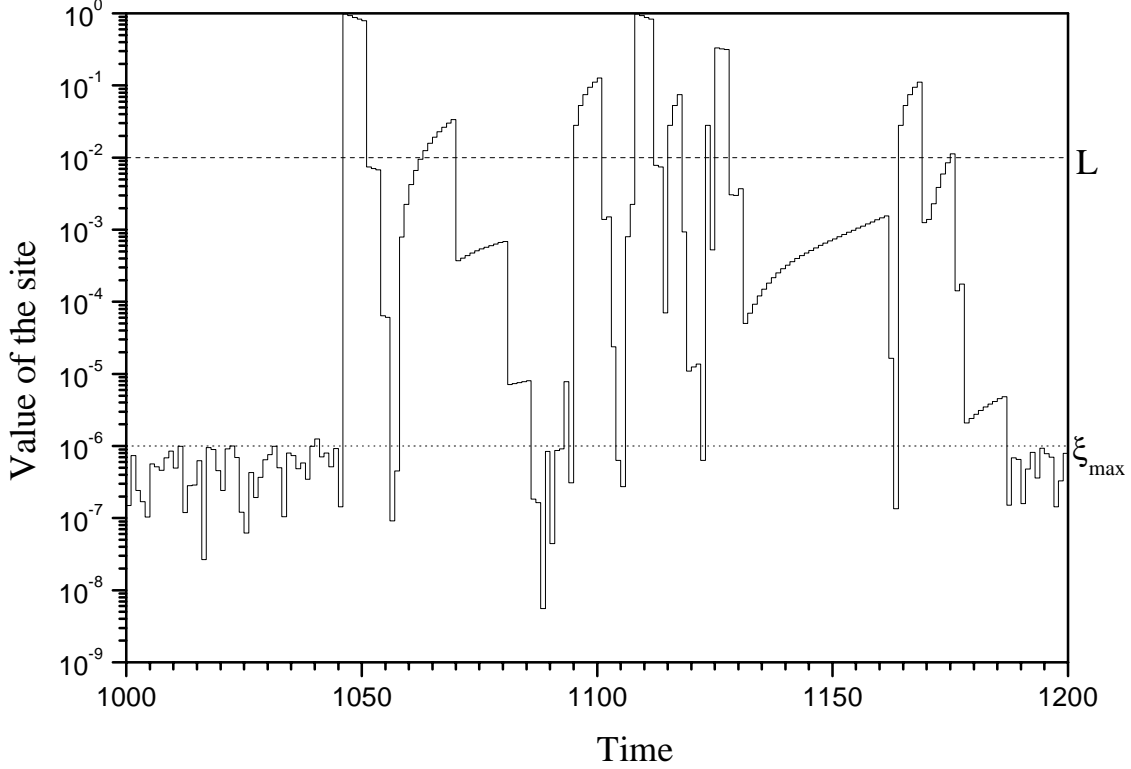
Figure 1: Temporal evolution of an arbitrary site (# 48), initiating from the noise domain below the noise threshold ξ_{max}, and later entering the region of "high" fitness given by *L.*

In Fig. 1 the time evolution due to Eq. (3) of one arbitrarily chosen site (i.e., site #48 in our case) is displayed together with the noise threshold ξ_{max} (dotted line) and the high fitness threshold *L* (dashed line). The two typical sources of high fitness values are seen as coming from i) boosts at time steps $t = 1046$ and $t = 1108$ up to a value of order $O(1)$ after normalization which lead to a stepwise decrease due to the diffusion rule (1) and a jumplike decrease due to the boost of some other site within the array and the subsequent suppression of the non-boosted sites by the factor $A_{amp} = 100$ due to the normalization procedure. The second source comes from contributions of neighbored large-valued sites leading to staircase-like increases of the site's values.

A spatiotemporal plot of all sites above the threshold value *L* is shown in Fig. 2. The fragments gather around a narrow array and are not distributed over the whole spatiotemporal plane as shown in Fig. 3. This effect represents a certain "taming" of evolutionary chance and comes from the restriction requiring that all sites be larger than the noise threshold $\xi_{max} = 10^{-6}$ for their possible enhancement. (As stated above, eventual values below the noise threshold thus contribute only to the noise itself, but cannot be boosted to values dominating the whole

evolution.) Since the range of those values which are checked by the ε-condition of (3) contains only six orders of magnitude, a boosted site will be placed in the spatial neighborhood of a fragment t_{mem} time steps ago. As will be shown in Section 3, this "stream-like" feature in the fitness landscape is crucial for the punctuated equilibrium behavior during the systems evolution.
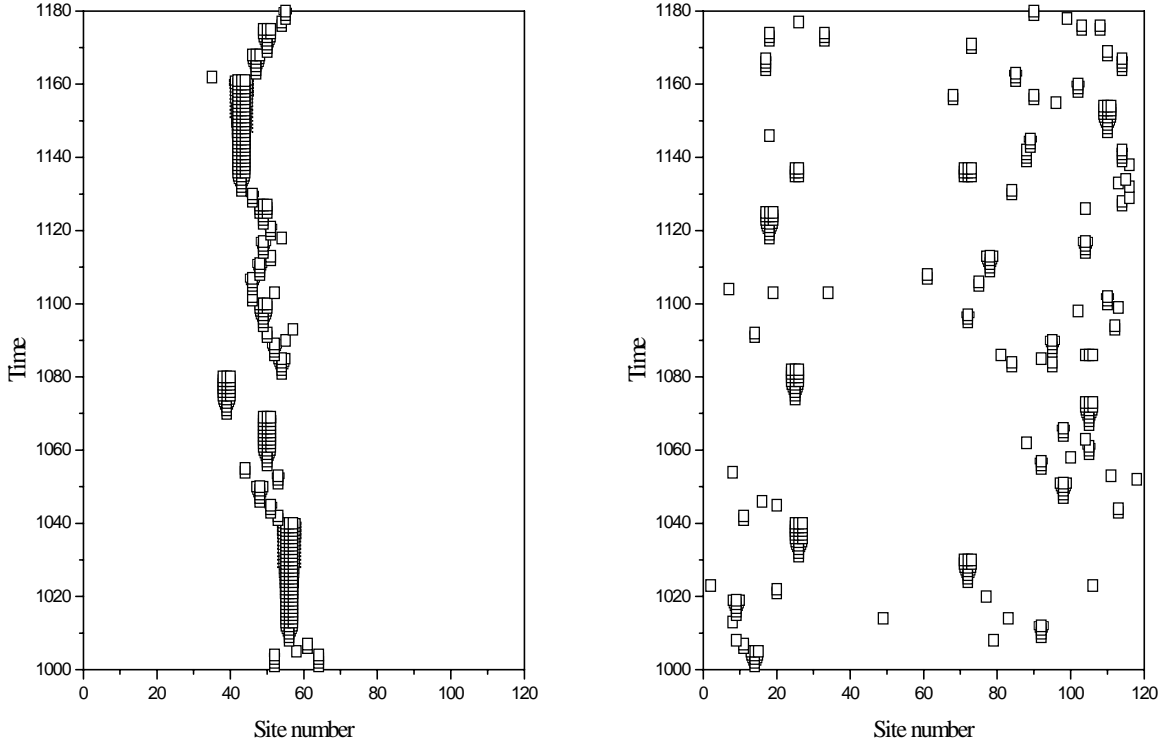
Figures 2 and 3: Density plot of the evolving system accentuating the range of the box values from $L = 10^{-2}$ to 10^{-1}. Values larger than 10^{-1} are displayed with the maximal box size. In Fig. 2, the noise threshold ξ_{max} is chosen as $\xi_{max} = 10^{-6}$. The distribution of fragments is constrained to a narrow domain. In the long-term evolution practically all regions of the array are reached by the stream of fragments in a random-walk-like manner. In Fig. 3, ξ_{max} is chosen as $\xi_{max} = 10^{-30}$. A similar pattern distribution is obtained at high values of ξ_{max} like, e.g., $\xi_{max} = 10^{-2}$ The consequences of this overall distribution are discussed in Section 3.

The analysis of the lifetimes of high fitness values for each site, i.e., with fitness values lying above the threshold value $\xi_{max} = 10^{-2}$ leads to a system's global property called "fractal evolution" (Fussy and Grössing, 1994; Fussy *et al.*, 1996a) which is also valid in our new version without global pattern analysis. The mean lifetime $\bar{\tau}$ of high fitness which is estimated in our new, simplified version by the arithmetic mean of all the maximal temporal extensions of all fragments for a chosen ε (in contrast to our former method of pattern analysis, where fragments were defined as connected regions with high fitness values) scales according

$$\bar{\tau} = a \cdot \varepsilon^b \ ,$$

$$\text{with} \quad a = 3.12 \pm 0.06, \, b = -0.590 \pm 0.005,$$

(5)

practically irrespective of variations of the systems variables or the initial conditions. Note that the power-law behavior of the parameter $\bar{\tau}$ with regard to the resolution-like parameter ε is not only valid for each "individual" site but also for the whole array. Therefore, we can speak of a system's order parameter $\bar{\tau}$ providing a dynamically invariant measure for the emerging spatiotemporal patterns given by the fractal evolution exponent b. As can be seen in Fig. 4, b remains constant for other chosen threshold values of high fitness.
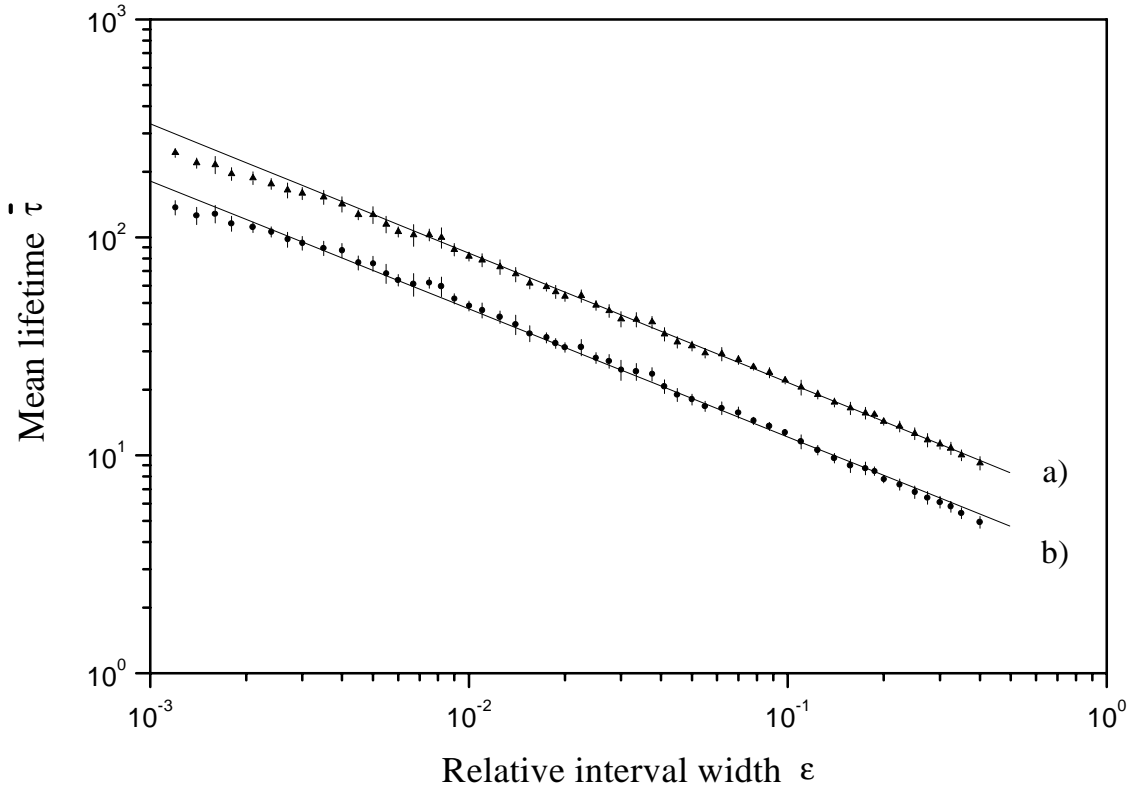
Figure 4: Log-log plot of the mean lifetimes $\bar{\tau}$ of the fragments versus the relative interval width ε for two values of the high fitness threshold L: a) $L = 10^{-4}$, b) $L = 10^{-2}$. The fractal evolution exponent which is estimated by the slope of the fit curve remains constant

2.2 Random Evolution

We have also analyzed a random version of the model presented in the former section. It is based on a Quantum Cellular Automaton introduced in Fussy *et al.* (1996a) and has been adapted for the biological context used here. In contrast to the memory-based selection criterion of Section 2.1, the potentially boostable sites are chosen randomly. Their fitness values only have to lie above the noise threshold ξ_{max}. The number of random boosts within a certain time interval T is given by R. For the default model, $T = 1000$ and $R = 160$ are chosen. That is, within the spatiotemporal plane $N \cdot T$, 160 lattice points $\left(j_{RAN}, t_{RAN} \right)$ with $1 \le j_{RAN} \le N, 1 \le t_{RAN} \le T$ are randomly chosen to be boosted. Note that this kind of boost generation represents, on one hand, a generalisation of the former mechanism, since with an appropriate random function one should be able to simulate also the outcome of the ε-based model. On the other hand, one looses the track of

7

the actual source(s) of the boost activites and has to be content with only a statistical description of potentially underlying reasons.

The complete evolution rule now reads as

$$\rho(t,j) = \frac{1}{N(t)} \Big\{ \big[A_{amp} - \rho_{0,\xi}(t,j)\big] \cdot \theta_\xi \cdot \delta_{j,j_{RAN}} \cdot \delta_{t,t_{RAN}} + \rho_{0,\xi}(t,j) \Big\}$$

with

$\rho_{0,\xi}(t,j)$, and θ_ξ defined in Eq. (3),

$1 \le j_{RAN}(T) \le N$, $nT \le t_{RAN} \le (n+1)T$, $n = 1,2,...$ (6)

We get similar results as shown in Figs. 1 to 4, but the power law (cf. Eq. (5)) is characterized now by a significantly different exponent b_R

$$\bar{\tau} = a_R \cdot R^{b_R} ,$$

with $a_R = 820 \pm 10$, $b_R = -0.930 \pm 0.003$. (7)

This difference and the absence of a complexity measure for the random model to be discussed in the following Section, are based on the fact that the pool of comparative values within the ε-based model does not contain perfect "white noise" terms due to the specific deterministic part of the evolution rule (3), cf. also Fussy *et al.* (1996a).

2.3 Hierarchically Emergent Fractal Evolution (HEFE)

Since fractal evolution in the true sense of the word is effectively realized only if the interval width ε or R, respectively, are allowed to acquire different values during the systems evolution, an additional long-term control cycle is imposed leading to an adaptive change of ε (or R) on the next higher level of the system's hierarchical nesting of feedback loops.

We discuss the mechanism with examples for the ε-based version. The random model is treated analogously by replacing ε by R. We let the system be driven by fluctuations of $\bar{\tau}_{exp}$ measured with the same ε during two succeeding long time spans or "generations" (*n, n+1*). The difference $\bar{\tau}_{exp}(n+1) - \bar{\tau}_{exp}(n)$ is practically always nonzero due to the finite time interval of data taking. To implement an adaptive change of ε or resolution 1/ε, respectively, of the whole fitness landscape, this difference is fed back into the consecutive value of ε via the difference quotient of the power-law (5)

$$\frac{\Delta\bar{\tau}}{\bar{\tau}} = b\frac{\Delta\varepsilon}{\varepsilon} ,$$

(8)

leading finally to

$$\varepsilon_{n+2} := \varepsilon_{n+1} = \varepsilon_n \left[1 + \frac{1}{b} \frac{\overline{\tau}_{n+1} - \overline{\tau}_n}{\overline{\tau}_n} \right].$$
(9)

As a main result, we obtain a progressive alteration of ε or the resolution 1/ε, respectively, within the system's evolution, a feature which has been denoted as "hierarchically emergent fractal evolution" (HEFE) (Fussy *et al.*, 1996b). In effect, HEFE constitutes a fluctuation driven and adaptive mechanism for the gradual increase of the mean lifetimes of high fitness values for each site/species. Consequently, a long-term growth of each species' lifetime and thus also of its complexity is obtained.
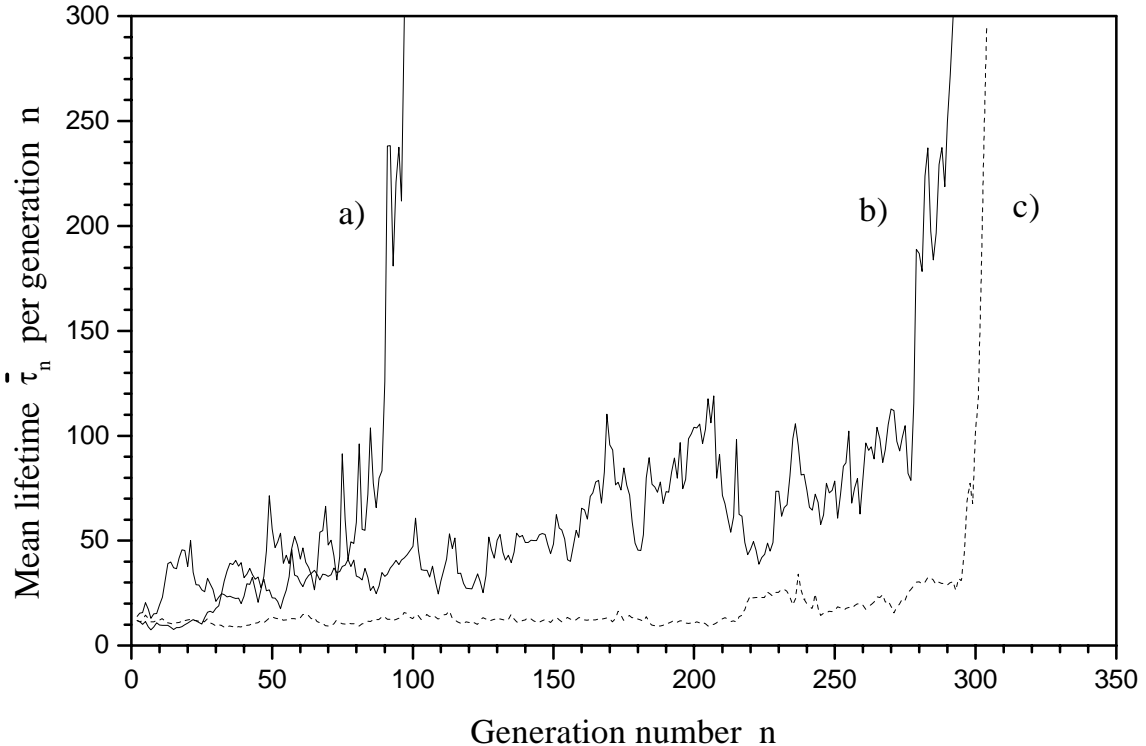
Figure 5: Hierarchically emergent fractal evolution (HEFE) for two different values of time spans of data taking ("generations") with particular ε in the memory model. The time span for each generation is given by 3000 time steps for curve a), and 5000 for curve b). The starting value of ε for both curves is $\varepsilon_0 = 10\,\%$. Curve c) shows the random case for a time span of 1000 time steps and with a starting value of $R = 100$. Apart from the obvious time asymmetry of the evolution, note also the characteristic stepwise increases as well as decreases of the mean lifetimes per generation, thus indicating two opposing trends in the short-term dynamics. In the long run, however, the mean lifetime is bound to increase.

In Fig. 5, two examples of temporal evolutions of the mean lifetimes per generation are shown for the memory-based model according to two different time spans of each generation during which the mean lifetime is determined. The third curve describes the evolution in the random model. Although fluctuations are allowed with equal opportunity for decreasing and increasing lifetimes, respectively, a long-term increase of the mean lifetimes is observed practically in all cases and has its origin in the functional property of the power-law (10). Denoting the deviation of the mean

lifetime by $\bar{\tau}_{n+1} - \bar{\tau}_n =: \eta^{\pm} \cdot \bar{\tau}_n$, and assuming one positive-valued deviation η^{+} for the consecutive generations ($n,n+1$) and a negative-valued one η^{-} of about equal size $\eta^{+} \approx -\eta^{-}$ for the succeeding ones ($n+2,n+3$), one obtains altogether a clear tendency towards decreasing relative interval widths

$$\varepsilon_{n+4} \approx \varepsilon_n \left[1 - \left| \frac{\eta^{\pm}}{b} \right|^2 \right] < \varepsilon_n , \tag{11}$$

leading to an average increase of the mean lifetime $\bar{\tau}$ per generation.

For relatively small time spans, i.e. for curve a) with 3000 time steps per generation, the fluctuation of the lifetimes is larger, of course, than for 5000 time steps. Therefore, the observed drastic increase of the mean lifetimes will occur sooner. In the random model an increase of the mean lifetimes for high fitness values is also observed (cf. curve c) in Fig. 5). Due to the more homogenous random distribution of boosts, the fluctuations are smaller, so for a generation length of 1000 time steps it takes already a relatively long time (almost 300 generations) until the mean lifetimes of high fitness values increase drastically. The common long-term growth of each species' lifetime of high fitness and thus also for its potential biological improvements can be interpreted as a coevolutionary "Red-Queen-effect" in the sense that each species has to "try hard" to *maintain* its relative position with respect to the remaining competing species by perpetually *changing* (and, finally, improving) its fitness within the ever changing fitness landscape.

To summarize, the point of our proposed mechanism of systems evolution breaking time symmetry lies in a perpetual multiplicative decrease of a parameter (ε or R, respectively) which is indirectly proportional to a complexity measure of the systems evolution, that is, the mean lifetimes for high fitness domains. Strictly speaking, since we analyze only a macroscopic level of biological evolution, a mechanism has been presented which leads to an increase for high fitness lifetimes for each species, enlarging thereby the probability for survival of the species and, consequently, also the probability for genetic improvement via mutational mechanisms at the level of microevolution.

3. Complexity Measures and the Role of Noise

In this section, other features of our toy model of macroevolution as mentioned in the introduction are discussed.

As can be seen from Fig. 2, the stream-like movement of high fitness domains through the whole array of species, at least in the long run, reflects an intermittent boost/mutation activity behavior of each site. That is, each site experiences an episodic evolution, where long periods of stasis are interrupted by bursts of rapid activity, a scenario called punctuated equilibrium (Eldredge and Gould, 1972; Gould and Eldredge, 1993). Moreover, since the observed activity is restricted to a relatively small domain of the whole spatial array, we can interpret the collective presence within low fitness domains for the remaining sites as kind of "coordinated stasis" (Kerr, 1997), which represents punctuated equilibrium at a higher level. Due to the random-walk-like movement of

the small activity regime across the whole array after an accordingly long time interval, practically each site/species gets the chance to obtain a high survival rate. Note that for very low *and* very high values of the background noise ξ_{max} (cf. Fig. 3), said properties disappear due to the uniform distribution of high fitness domains all over the fitness landscape.
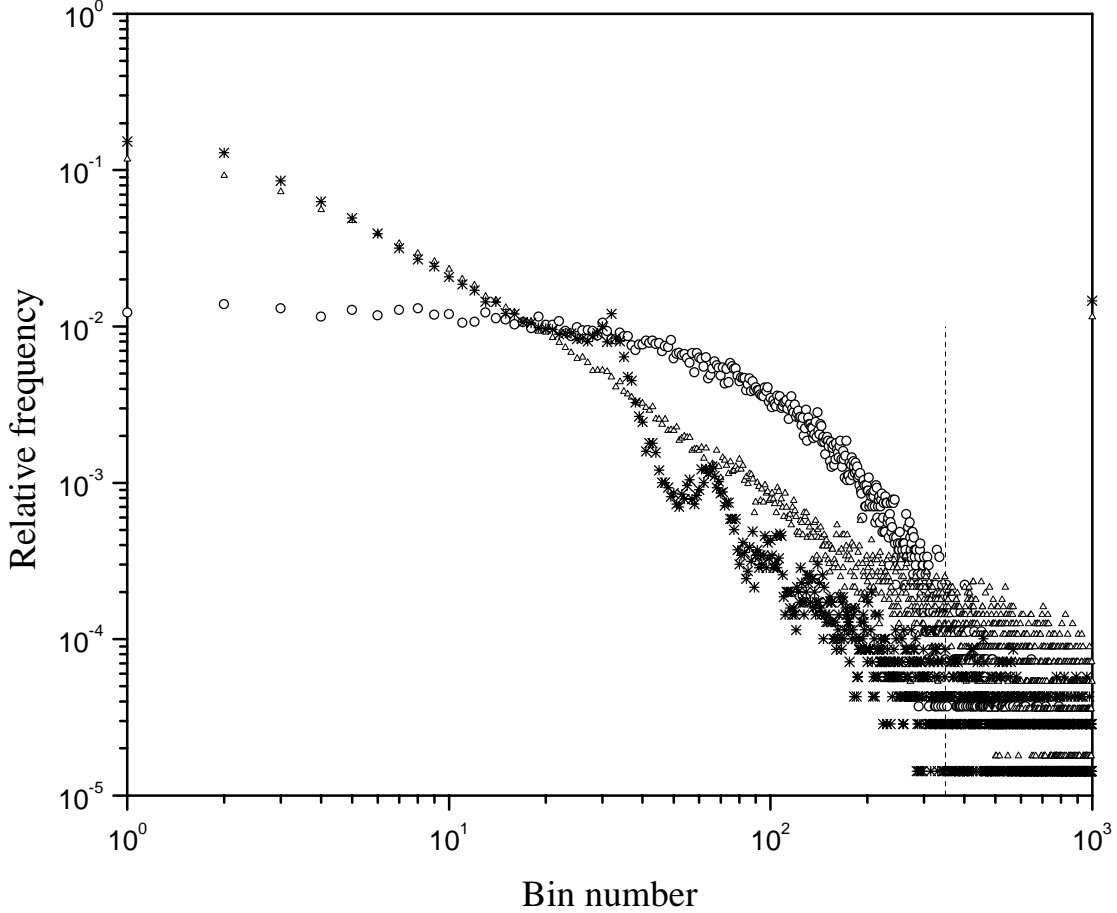
Figure 6: Relative frequency distribution of the sizes of the time plateaus, i.e. the periods of stasis, according to their size for two values of the background noise. The plateau sizes for both the memory and the random model at $\xi_{max} = 10^{-6}$ are present on all length scales, and their frequency scales with a power law. However, for $\xi_{max} = 10^{-40}$ (circled data), a sharp cutoff (dashed line) of plateau sizes for higher bin numbers is observed

To quantify this feature, we have plotted in Fig. 6 the relative frequency distribution of the periods of stasis (i.e., the time span between two consecutive boosts) with respect to their size, which is represented by bin numbers with a bin width of 10. Bin #10, e.g., contains all sizes from 90 to 99. Bin #1000 contains the sizes 9990 to 9999 and, additionally, all other ones larger than 9999. The plateau sizes *s* for both the memory and the random model at $\xi_{max} = 10^{-6}$ are present on all length scales and their frequency *f(s)* scales with a power law $f(s) \propto s^{-1.4}$ thus indicating a randomized devil's staircase function (Boettcher and Paczuski, 1996). However, for $\xi_{max} = 10^{-40}$ which simulates practically the noise-free case, a sharp cutoff of plateau sizes for higher bin numbers is observed. This breakdown of the scaling behavior takes also place in the memory-

11

based model for high values of ξ_{max} indicating the dominant role of background noise under the aspect of system affecting control parameters.

In the following, a quantitative measure is introduced to account for the different complexity states. It has turned out that the "usual" measure of the disorder of a system's state, the relative Shannon information entropy

$$\frac{S}{S_{max}} = \frac{-1}{\ln N} \sum_{j=1}^{N} \rho(t,j) \cdot \ln \rho(t,j) \qquad (12)$$

represents an inappropriate measure with regard to an overall statement about the system's complexity. In Fig. 7, the entropy, summed over 50000 time steps and normalized, exhibits for both the memory and the random model a monotonous behavior with regard to the variation of the noise level.
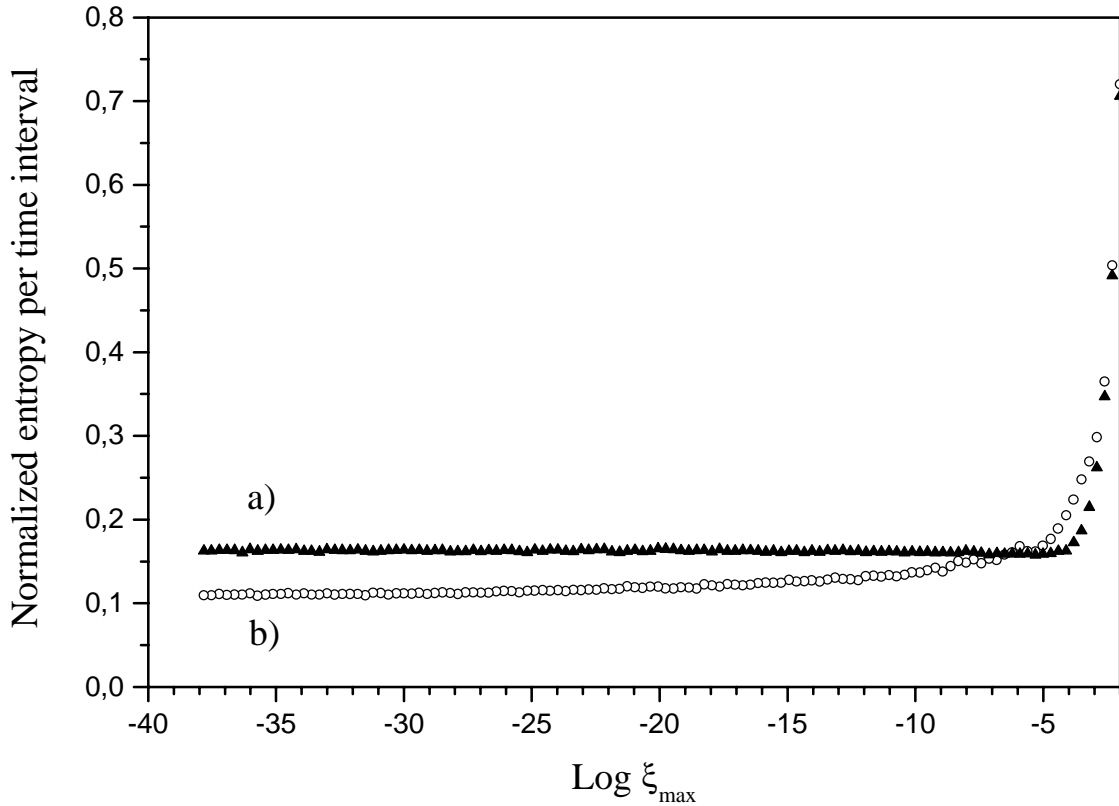
Figure 7: Normalized entropy within a time interval of 50000 time steps versus the underlying noise threshold ξ_{max} for a) the random model and b) the memory-based model. The entropy increases monotonically over a range of almost 40 orders of magnitude

An appropriate measure to account for the phenomena listed above was found in a variable indicating the boost distribution on the spatiotemporal plane. The spatial distance of two consecutively boosted sites $\rho_b(t,j)$ and $\rho_{b+1}(t',j)$ reads as $w_{b,b+1}(i,j) = \min\left(|i-j|, \||i-j|-N|\right)$

12

due to the periodic boundary conditions. They are summed up for all occurring boosts, with their total number equaling $B(\Delta t)$ within a certain time span Δt. The mean value $\overline{w}$ of the obtained spatial distances $w_{b,b+1}(i,j)$ is finally given by

$$\overline{w} = \frac{1}{B-1}\sum_{b=1}^{B-1} w_{b,b+1} \ .$$ (13)
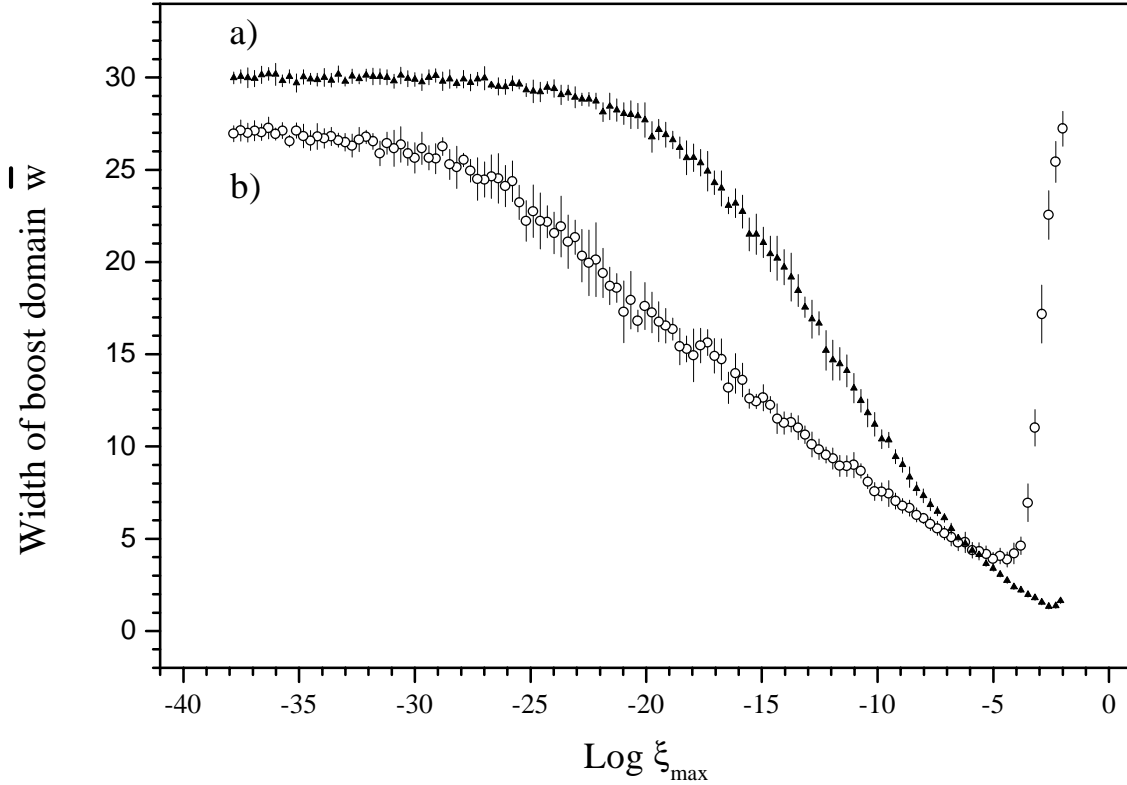
Figure 8: The mean width of the boost domain as a quantitative measure of the complexity of the system for a) the random model and b) the memory-based model. The minimum of $\overline{w}$ for b) indicates the range of background noise which leads to narrow boost domains and thus to the most complex system's behavior.

By calculating the mean spatial distance $\overline{w}$ for different values of ξ_{max} we obtained a gradual, convex-shaped change of $\overline{w}(\xi_{max})$ for the memory-based model as shown in Fig. 8. Each data point was obtained by measuring the boost distances for a time span of $\Delta t = 20000$ time steps. At the minimum of $\overline{w}(\xi_{max})$ obtained with ξ_{max} between 10^{-4} and 10^{-6}, we indeed observe the stream-like behavior of the boost domains (cf. Fig. 2), and, consequently, the most complex system's behavior. For very low and very high values of ξ_{max} the mean boost distance comes close to the value obtained for randomly distributed patterns. Note that we have used in our case $N = 120$ sites and periodic boundary conditions. Therefore, the maximal spatial boost distance amounts to $N/2 = 60$. In the random case, which is almost, but not exactly fulfilled in our system due to our deteministic rules, the mean distance then amounts to the mean value, i.e. $\overline{w}_{random} \approx 30$ (cf. curve a) in Fig.8). The reason for the existence of a mimimum of $\overline{w}$ in the memory-based

model and its absence in the random case lies in the comparison procedure for each site with the past one. For high values of the background noise the signal to noise ratio has decreased to such an amount, that the probabilty for the noise values to fulfill the ε-condition in Eq. (3) has increased dramatically. Consequently, the whole array of the sites is potentially boostable. In the random model, the boostable sites are chosen randomly from the signal-like small domain of sites above the noise threshold, and thus the actually boosted sites remain restricted to said domain.

Note that at the maximal noise level of $\xi_{max} = 10^{-2}$ practically all features like fractal evolution, HEFE and punctuated equilibrium (the latter one only for the memory-based model) break down. The convex shape of curve b) in Fig. 8 indeed can be interpreted as "second-order" complexity measure (Atmanspacher *et al.,* 1997), which filters out those systems states exhibiting the most "interesting" in the sense of most complex sytems properties.

4. Conclusions

We have presented a further developed and (with respect to random boost generation) generalized model of progressive evolution at a macroscopic level, as first introduced in Fussy *et al.* (1997).

The proposed concept of hierarchically emergent fractal evoluion (HEFE) leads to the potential development of individual species towards gradually higher complexity as represented by an evolution towards higher values of mean fitness lifetimes. The HEFE mechanism can thus be interpreted such that a single species is constantly engaged, via the possibilities of beneficial selection versus detrimental extinction, in a struggle for higher fitness values, while there exists a "Red-Queen-effect" also as global tendency of ever higher fitness values to emerge for the whole ensemble of species. Our model therefore avoids the problems arising with models for macroevolution based on self-organized criticality, where a "quasi - steady state" is reached with no time-irreversible evolution.

It has turned out that the parameter ξ_{max} characterizing the maximal noise background plays a crucial role for the systems evolution and its derived measures. We have shown that for certain ranges of the values of the systems parameters, the number of emerging robust system features becomes maximal. To those features belong fractal evolution via a temporal feedback process, punctuated equilibrium and the potential growth of complexity for each species via the HEFE mechanism, as well as their "quality", i.e., their validity over a wide range of the systems parameters' values.

If the parameter characterizing the maximal noise background is taken as control parameter and varied over a range of many orders of magnitude, some or all complex features gradually vanish. At both extremes of noise level values, the memory-based system exhibits similar, random-like properties, which are not adequately described by the usual entropy measure, since the latter one grows monotonically with growing noise level. However, a variable characterizing the mean spatial distance of consecutive evolutionary activity events within the one-dimensional array of sites/species enables an appropriate description of the system's reduced and maximal complexity. The random model does not possess that complexity indicating parameter like the memory-based model, but it exhibts all complex features like HEFE and punctuatd equilibrium without the need of an additional systems memory.

References

Bak Per and Sneppen Kim (1993). Punctuated equilibrium and criticality in a simple model of evolution, *Phys. Rev. Lett.* **71** (1993) pp. 4083-4086.

Bak Per, Tang Chao and Wiesenfeld Kurt (1987, 1988). Self-organized criticality: an explanation of *1/f* noise, *Phys. Rev. Lett*. **59** (1987) pp. 381-384, Self-organized criticality, *Phys. Rev*. **A38** (1988) pp. 364-374.

Boettcher Stefan and Paczuski Maya (1996). Exact results for spatiotemporal correlations in a self-organized critical model of punctuated equilibrium, *Phys. Rev. Lett*. **76** (1996) pp. 348-351.

Eldredge Niles and Gould Stephen Jay (1972). Punctuated equilibria: An alternative to phylogenetic gradualism, in *Models in Paleobiology*, ed. by T.J.M. Schopf. Freeman, San Francisco.

Fussy Siegfried and Grössing Gerhard (1994). Fractal evolution of normalized feedback systems on a lattice. *Phys. Lett*. **A186** (1994) pp. 145-151.

Fussy Siegfried, Grössing Gerhard and Schwabl Herbert (1996a). Fractal evolution in deterministic and random models. *Int. J. Bifurcation and Chaos* **6** (11) (1996) pp. 1977-1995.

Fussy Siegfried, Grössing Gerhard and Schwabl Herbert (1996b). Hierarchically emergent fractal evolution. In *Cybernetics & Systems '96 Vol. I* , ed. by Trappl R. (Vienna, 1996) pp.189-194.

Fussy Siegfried, Grössing Gerhard, and Schwabl Herbert (1997). A simple model for the evolution of evolution. *Journal of Biological Systems* , **5** (3) (1997) pp. 341-357.

Gordon Richard (1998). The Hierarchical Genome and Differentiation Waves: Novel Unification of Development, Genetics, and Evolution. World Scientific, Singapore. In press (1998).

Gould Stephen Jay and Eldredge Niles (1993). Punctuated equilibrium comes of age, *Nature* **366** (1993) pp. 223-227.

Gould Stephen Jay (1996). Full House. The Spread of Excellence from Plato to Darwin. Crown. New York (1996).

Kauffman Stuart A. (1993). The Origins of Order. Oxford Univ. Press, New York Oxford (1993).

Kerr Richard A. (1997). Does Evolutionary History Take Million-Year Breaks? *Science* **278** (1997), pp. 576-577.

Robertson Douglas S. and Grant Michael C. (1996). Feedback and chaos in Darwinian evolution. *Complexity* **2** (1) (1996), pp. 10-14.

Schuster Peter (1994). Molekulare Evolution an der Schwelle zwischen Chemie und Biologie. In *Die Evolution der Evolutionstheorie*, ed. by Wieser W., Spektrum Akademie Verlag, Heidelberg-Berlin-Oxford (1994) pp. 49-76.

Smith John Maynard and Szathmáry Eörs (1997). The Major Transitions in Evolution. Oxford University Press (1997).

Solé Richard V. and Manrubia Susanna C. (1996). Extinction and self-organized criticality in a model of large-scale evolution. *Phys. Rev*. **E54** (1996) pp. R42-R45.

Vandewalle Nicolas and Ausloos Marcel (1995). Self-organized criticality in phylogenetic-like tree growths. *J. Phys. I France* **5** (1995) pp. 1011-1025.